

# Ground State Phase Diagram of $S = 1$ Diamond Chains

Kazuo HIDA\* and Ken'ichi TAKANO<sup>1</sup>

*Division of Material Science, Graduate School of Science and Engineering,  
Saitama University, Saitama, Saitama 338-8570*

<sup>1</sup>*Toyota Technological Institute, Tenpaku-ku, Nagoya 468-851*

(Received November 27, 2018)

We investigate the ground-state phase diagram of a spin-1 diamond chain. Owing to a series of conservation laws, any eigenstate of this system can be expressed using the eigenstates of finite odd-length chains or infinite chains with spins 1 and 2. The ground state undergoes quantum phase transitions with varying  $\lambda$ , a parameter that controls frustration. Exact upper and lower bounds for the phase boundaries between these phases are obtained. The phase boundaries are determined numerically in the region not explored in the previous work [Takano *et al.* J. Phys.: Condens. Matter **8** (1996) 6405].

arXiv:1611.10050v1 [cond-mat.str-el] 30 Nov 2016

## 1. Introduction

The quantum effects in frustrated magnets have been extensively studied in condensed matter physics.<sup>1</sup> The interplay of quantum fluctuation and frustration gave birth to various exotic quantum phases. Among a variety of models and materials with strong frustration, the diamond chain, that consists of successive diamond-shaped units as depicted in Fig. 1, has been attracting the interest of many condensed matter physicists. In addition to the well-known natural mineral azurite<sup>2,3</sup> which is a spin-1/2 distorted diamond chain, it is pointed out quite recently that  $[\text{Ni}_3(\text{OH})_2(\text{O}_2\text{C}-\text{C}_2\text{H}_2-\text{CO}_2)(\text{H}_2\text{O})_4]\text{E}2\text{H}_2\text{O}$ <sup>4</sup> can be regarded as a spin-1 distorted diamond chain.<sup>5,6</sup>

From the theoretical viewpoint, the diamond chain is remarkable, since it has been rigorously treated to some extent in the absence of distortion.<sup>7</sup> The ground state phases of the spin-1/2 diamond chain are fully understood. The distorted version of this model with spin 1/2 has also been intensively investigated theoretically<sup>8,9</sup> as a model for azurite. The case of mixed spin diamond chain with  $S = 1/2$  and 1, which has a Haldane-type ground state in the absence of frustration, has been also extensively studied theoretically.<sup>10-13</sup>

The case of higher spin uniform diamond chain has been briefly discussed in Ref. 7. With the increase of spin magnitude, much richer phase diagrams than the case of spin-1/2 are expected. However, the full phase diagram has not yet been obtained even for the case of  $S = 1$ . We expect that the discovery of the spin-1 distorted diamond chain material<sup>6</sup> opens a new field in the physics of frustrated quantum magnetism, since the ground state of ideal spin-1 diamond chains not only have richer phases compared to the spin-1/2 case but also can generate even more variety of phases in the presence of realistic perturbations such as lattice distortion, anisotropy, and inter-chain coupling. Motivated by this speculation, we de-

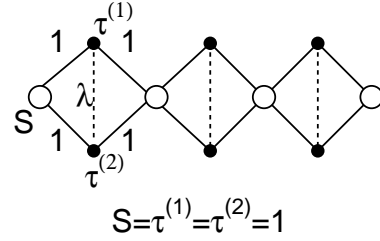


Fig. 1. Structure of the diamond chain.

termine the complete ground-state phase diagram of the ideal spin-1 diamond chain based on the exact wave function in the present work.

This paper is organized as follows. In the next section, the model Hamiltonian is presented and the structure of the eigenstates is explained. The possible ground states are proposed in Sect. 3. The exact upper and lower bound for the phase boundaries are discussed in Sect. 4. The phase boundaries are numerically determined in Sect. 5. The last section is devoted to the summary and discussion.

## 2. Hamiltonian and Cluster Eigenstates

The Hamiltonian of the  $S = 1$  diamond chain in Fig. 1 is represented as

$$\mathcal{H} = \sum_{l=1}^L \left[ \mathbf{S}_l \boldsymbol{\tau}_l^{(1)} + \mathbf{S}_l \boldsymbol{\tau}_l^{(2)} + \boldsymbol{\tau}_l^{(1)} \mathbf{S}_{l+1} + \boldsymbol{\tau}_l^{(2)} \mathbf{S}_{l+1} + \lambda \boldsymbol{\tau}_l^{(1)} \boldsymbol{\tau}_l^{(2)} \right], \quad (2.1)$$

where  $\mathbf{S}_l$  (hereafter called  $S$ -spin) and  $\boldsymbol{\tau}_l^{(\alpha)}$  ( $\alpha = 1, 2$ ) (called  $\tau$ -spin) are spin operators with magnitude 1 in the  $l$ th unit cell. The bond connecting the spins  $\boldsymbol{\tau}_l^{(1)}$  and  $\boldsymbol{\tau}_l^{(2)}$  are called diagonal bonds.

By defining the composite spin (called  $T$ -spin)  $\mathbf{T}_l \equiv$

\*E-mail: hida@mail.saitama-u.ac.jp

$\tau_l^{(1)} + \tau_l^{(2)}$  for all  $l$ , Hamiltonian (2.1) is also expressed as

$$\mathcal{H} = \sum_{l=1}^L \left[ \mathbf{S}_l \mathbf{T}_l + \mathbf{T}_l \mathbf{S}_{l+1} + \frac{\lambda}{2} (\mathbf{T}_l^2 - 4) \right]. \quad (2.2)$$

In this representation, it is clear that  $\mathbf{T}_l^2$  ( $l = 1, 2, \dots, L$ ) commutes with  $\mathcal{H}$ . Hence,  $T_l$  defined by  $\mathbf{T}_l^2 = T_l(T_l + 1)$  is a good quantum number that takes the values 0, 1 and 2. Thus, within the sector specified by the sequence of  $T$ -spin magnitudes  $\{T_l\}$ , the Hamiltonian (2.2) is equivalent to the following Hamiltonian

$$\mathcal{H}(\{T_l\}, \lambda) = \tilde{\mathcal{H}}(\{T_l\}) + \frac{\lambda}{2} \sum_{l=1}^L (T_l + 1)T_l - 2L\lambda, \quad (2.3)$$

where  $\tilde{\mathcal{H}}(\{T_l\})$  is the Hamiltonian of the mixed spin antiferromagnetic Heisenberg chain (MAFH) defined by

$$\tilde{\mathcal{H}}(\{T_l\}) = \sum_{l=1}^L [\mathbf{S}_l \mathbf{T}_l + \mathbf{T}_l \mathbf{S}_{l+1}] \quad (2.4)$$

with fixed  $T$ -spin magnitudes  $\{T_l\}$ .

If  $T_l = 0$ , the  $\tau$ -spins on the  $l$ th diagonal bond form a singlet pair, which we call a dimer. The dimer breaks the correlation between the  $S$ -spins on the both sides. The ground state of the finite chain consisting of  $S$ -spins and  $\tau$ -spins in the region between two dimers is called a cluster- $n$ , if the region includes  $n$  diagonal bonds and all  $T$ -spins on them are nonzero. A cluster- $n$  is specified by an  $n$ -membered subsequence  $\{T_l\}_{i,n} \equiv \{T_i \cdots T_{i+n-1}\}$  of  $\{T_l\}$  with  $T_l = 1$  or 2. The cluster- $n$  with the sequence  $\{T_l\}_{i,n}$  is the ground state of the Hamiltonian

$$\mathcal{H}(\{T_l\}_{i,n}) = \tilde{\mathcal{H}}(\{T_l\}_{i,n}) + \frac{\lambda}{2} \sum_{l=i}^{i+n-1} [(T_l + 1)T_l - 4] \quad (2.5)$$

with

$$\tilde{\mathcal{H}}(\{T_l\}_{i,n}) = \sum_{l=i}^{i+n-1} [\mathbf{S}_l \mathbf{T}_l + \mathbf{T}_l \mathbf{S}_{l+1}], \quad (2.6)$$

which is the Hamiltonian for the MAFH with  $2n + 1$  spins and the open boundary condition. We denote the lowest eigenvalues of (2.5) and (2.6) by  $E_G(\{T_l\}_{i,n}, \lambda)$  and  $\tilde{E}_G(\{T_l\}_{i,n})$ , respectively. They satisfy the relation

$$E_G(\{T_l\}_{i,n}, \lambda) = \tilde{E}_G(\{T_l\}_{i,n}) + \frac{\lambda}{2} \sum_{l=i}^{i+n-1} [(T_l + 1)T_l - 4]. \quad (2.7)$$

The lowest eigenstate of the total Hamiltonian (2.3) with fixed  $\{T_l\}$  is a tensor product of dimers at zero  $T$ -spins and of cluster- $n$ 's between them. If the state include

$N_c$  cluster- $n$ 's, the lowest eigenvalue is written as

$$E_G^{\text{tot}}(\{T_l\}, \lambda) = \sum_{\alpha=1}^{N_c} E_G(\{T_l\}_{i_\alpha, n_\alpha}, \lambda) - 2\lambda(N_c - 1), \quad (2.8)$$

where  $\{T_l\}_{i_\alpha, n_\alpha}$  is the sequence of nonzero  $T_l$  in the  $\alpha$ th cluster- $n$ .

### 3. Ground States

The ground state is a uniform array of cluster- $n$ 's with a common value of  $n$  and dimers in between. This state is called the dimer-cluster- $n$  (DC $n$ ) state. The DC0 state is also called the dimer-monomer state. In the DC $n$  phase, we can take  $T_{(n+1)p+q} = 0$  and  $\{T_l\}_{i,n} = \{T_l\}_n \equiv \{T_1 \dots T_n\}$  for  $i = (n+1)p + q + 1$  with all integer  $p$ . The integer  $q$  can be chosen arbitrarily within the range  $0 \leq q \leq n$ . Hence, this ground state has a spatial periodicity of  $n+1$  with the  $(n+1)$ -fold spontaneous translational symmetry breakdown.

The value of  $n$  and configuration  $\{T_l\}_n$  is determined so as to minimize the total energy for each  $\lambda$ . The energy per unit cell of the lowest energy state among the DC $n$  states is given by

$$\epsilon_G(\lambda) = \min_{n, \{T_l\}_n} \frac{1}{n+1} [E_G(\{T_l\}_n, \lambda) - 2\lambda]. \quad (3.1)$$

The phase boundary  $\lambda_c(n; \{T_l\}_n, \{T'_l\}_n)$  between the DC $n$  phases with  $T$ -spin configurations  $\{T_l\}_n$  and  $\{T'_l\}_n$  is given by

$$\begin{aligned} \lambda_c(n; \{T_l\}_n, \{T'_l\}_n) &= \frac{2(\tilde{E}_G(\{T'_l\}_n) - \tilde{E}_G(\{T_l\}_n))}{\sum_{l=1}^n [(T_l + 1)T_l - (T'_l + 1)T'_l]}. \end{aligned} \quad (3.2)$$

If  $T_l \neq 0$  for all diagonal bonds, the ground state energy of (2.1) per unit cell  $\epsilon_G(\infty, \{T_l\}, \lambda)$  can be expressed by the ground state energy  $\tilde{\epsilon}_G(\{T_l\})$  of the infinite MAFH with configuration  $\{T_l\}$  and  $\{S_l\}$  as

$$\epsilon_G(\infty, \{T_l\}, \lambda) = 2\tilde{\epsilon}_G(\{T_l\}) + \frac{\lambda}{2} \overline{(T_l + 1)T_l} - 2\lambda, \quad (3.3)$$

where

$$\overline{(T_l + 1)T_l} = \lim_{L \rightarrow \infty} \frac{1}{L} \sum_{l=1}^L (T_l + 1)T_l \quad (3.4)$$

is the average of  $(T_l + 1)T_l$  over the whole chain.

In Ref. 7, the following results are derived:

- (1) For  $\lambda > 2$ ,  $T_l = 0$  or 1 for all  $l$ . The ground state is the dimer-monomer (DC0) phase for  $\lambda > 3$ , tetramer-dimer (DC1) phase for  $2.660 \lesssim \lambda < 3$ , heptamer-dimer (DC2) phase for  $2.583 \lesssim \lambda \lesssim 2.660$ , DC3 phase for  $2.577 \lesssim \lambda \lesssim 2.583$  and DC $\infty$  phase for  $2 < \lambda < 2.577$ . In all these phases, the  $T_l = 1$  for all diagonal bonds in cluster- $n$ . Especially, the DC $\infty$  phase is the spin-1 Haldane phase.
- (2) For  $\lambda < 0$ ,  $T_l = 2$  for all  $l$ . Hence, the ground state

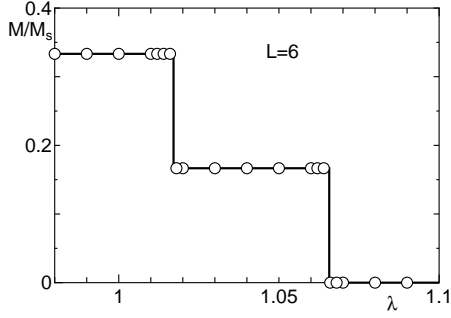


Fig. 2. Ground state magnetization for  $L = 6$ .

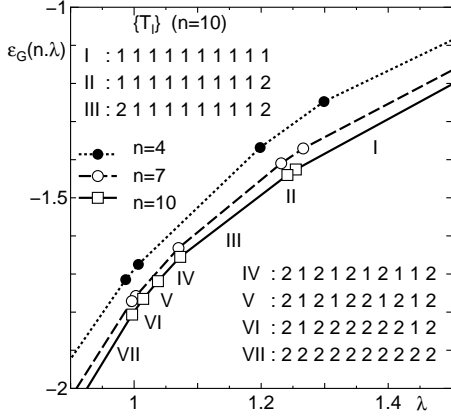


Fig. 3. Lowest energies of the  $DC_n$  states.

is ferrimagnetic with magnetization  $M = L$ .

However, the ground states for  $0 < \lambda < 2$  remained unresolved. In the present work, we determine the ground-state phases in this region.

To start with, we present the total magnetization  $M$  in the ground state obtained by numerical exact diagonalization of the whole chain with  $L = 6$  with periodic boundary condition. The results are shown in Fig. 2. We find  $M = M_s/3$  for  $\lambda \lesssim 1.0171$ ,  $M = M_s/6$  for  $1.0171 \lesssim \lambda \lesssim 1.0657$ , and  $M = 0$  for  $\lambda \gtrsim 1.0657$  where  $M_s (= 3L)$  is the saturated magnetization. No ground states with other values of magnetizations are found.

To identify the ground state phases in more detail, we estimate the ground state energy assuming the  $DC_n$  state with  $n \leq 10$  for all possible configurations  $\{T_l\}_n$ . The lowest energies of the  $DC_n$  states per site are plotted against  $\lambda$  in Fig. 3 for several values of  $n$  using the numerical exact diagonalization and finite size DMRG methods. In the DMRG calculation, the number  $m$  of states kept in each subsystem is 240. The convergence with respect to  $m$  is confirmed. The lowest energy of the  $DC_n$  state decreases with  $n$ . This suggests that the true ground state is the  $DC_\infty$  phase.

To get more insight into the configuration of  $\{T_l\}$  in the thermodynamic limit, we identify the configuration

$\{T_l\}_n$  in the  $DC_n$  state with finite  $n$  in more detail. For example, in the  $DC_{10}$  phase, there are six regions with different lowest energy configurations as shown in Fig. 3. However, the configurations in regions II and III differ from that in region I only locally. Similarly, the configurations in regions V and VI differ from that in region VII only locally. Hence, we speculate that the candidates of the configurations in the ground state  $DC_\infty$  phases are the following three configurations.

(1) Haldane phase

$$\{T_l\} = \{\dot{1}\}. \quad (3.5)$$

(2) Ferrimagnetic phase with  $M = M_s/6$  ( $F_{1/6}$  phase)

$$\{T_l\} = \{\dot{1}\dot{2}\}. \quad (3.6)$$

(3) Ferrimagnetic phase with  $M = M_s/3$  ( $F_{1/3}$  phase)

$$\{T_l\} = \{\dot{2}\}. \quad (3.7)$$

Here  $\{\dot{T}_1 \cdots \dot{T}_l\}$  denotes the configuration consisting of a periodic array of  $T_1 \cdots T_l$  over the whole chain.

#### 4. Upper and Lower Bounds for Phase Boundaries

To obtain the upper and lower bounds for the phase boundaries, we divide the whole Hamiltonian (2.2) as

$$\mathcal{H} = \mathcal{H}_n + \bar{\mathcal{H}}_n \quad (4.1)$$

where

$$\mathcal{H}_n = \sum_{l=i}^{i+n-1} \left[ \mathbf{S}_l \mathbf{T}_l + \mathbf{T}_l \mathbf{S}_{l+1} + \frac{\lambda}{2} (\mathbf{T}_l^2 - 4) \right] \quad (4.2)$$

and  $\bar{\mathcal{H}}_n$  is the remainder of  $\mathcal{H}$ . Consider an eigenstate of the whole diamond chain  $|\Phi(\{T_l\})\rangle$  specified by  $\{T_l\}$  that contains a sequence  $\{T_l\}_{i,n}$  with  $T_l \neq 0$  ( $i \leq l \leq i+n-1$ ). The expectation value of the total Hamiltonian with respect to  $|\Phi(\{T_l\})\rangle$  is expressed as

$$\langle \Phi(\{T_l\}) | \mathcal{H} | \Phi(\{T_l\}) \rangle = \langle \Phi(\{T_l\}) | \mathcal{H}_n | \Phi(\{T_l\}) \rangle + \langle \Phi(\{T_l\}) | \bar{\mathcal{H}}_n | \Phi(\{T_l\}) \rangle. \quad (4.3)$$

The following inequality holds in general,

$$\langle \Phi(\{T_l\}) | \mathcal{H}_n | \Phi(\{T_l\}) \rangle \geq \langle \Phi_n(\{T_l\}_{i,n}) | \mathcal{H}_n | \Phi_n(\{T_l\}_{i,n}) \rangle = \bar{E}_G(\{T_l\}_{i,n}) + \frac{\lambda}{2} \sum_{l=i}^{i+n-1} (T_l + 1)T_l - 2n\lambda, \quad (4.4)$$

where  $|\Phi_n(\{T_l\}_{i,n})\rangle$  is the lowest energy eigenstate of  $\mathcal{H}_n$  with configuration  $\{T_l\}_{i,n}$ . Similarly, we have an inequality,

$$\langle \Phi(\{T_l\}) | \bar{\mathcal{H}}_n | \Phi(\{T_l\}) \rangle \geq \bar{E}_G, \quad (4.5)$$

where  $\bar{E}_G$  is the ground-state energy of  $\bar{\mathcal{H}}_n$ .

Consider the lowest energy state  $|\Phi_0(\{T'_l\})\rangle$  of the Hamiltonian (2.2) within the sector specified by the sequence  $\{T'_l\}$  in which the subsequence  $\{T_l\}_{i,n}$  of  $\{T_l\}$

is replaced by a sequence  $\{T'_l\}_{i,n} = \{0T'_{i+1}\dots T'_{i+n-2}0\}$ . Note that  $T'_i = T'_{i+n-1} = 0$  by definition. The zeros on both ends breaks the correlation between the spins in  $\mathcal{H}_n$  and those in  $\bar{\mathcal{H}}_n$ . Then  $|\Phi_0(\{T'_l\})\rangle$  can be expressed as

$$|\Phi_0(\{T'_l\})\rangle = |\Phi_n(\{T'_l\}_{i,n})\rangle \otimes |\bar{\Phi}\rangle, \quad (4.6)$$

where  $|\bar{\Phi}\rangle$  is the ground state of  $\bar{\mathcal{H}}_n$  which satisfies

$$\bar{\mathcal{H}}_n |\bar{\Phi}\rangle = \bar{E}_G |\bar{\Phi}\rangle. \quad (4.7)$$

The expectation value of the total Hamiltonian with respect to  $|\Phi_0(\{T'_l\})\rangle$  is given by

$$\begin{aligned} \langle \Phi_0(\{T'_l\}) | \mathcal{H} | \Phi_0(\{T'_l\}) \rangle &= \langle \Phi_0(\{T'_l\}) | \mathcal{H}_n | \Phi_0(\{T'_l\}) \rangle \\ &+ \langle \Phi_0(\{T'_l\}) | \bar{\mathcal{H}}_n | \Phi_0(\{T'_l\}) \rangle, \end{aligned} \quad (4.8)$$

where

$$\begin{aligned} \langle \Phi_0(\{T'_l\}) | \mathcal{H}_n | \Phi_0(\{T'_l\}) \rangle &= \langle \Phi_n(\{T'_l\}_{i,n}) | \mathcal{H}_n | \Phi_n(\{T'_l\}_{i,n}) \rangle \\ &= \tilde{E}_G(\{T'_l\}_{i+1,n-2}) + \frac{\lambda}{2} \sum_{l=i+1}^{i+n-2} (T'_l + 1)T'_l - 2n\lambda, \end{aligned} \quad (4.9)$$

$$\langle \Phi_0(\{T'_l\}) | \bar{\mathcal{H}}_n | \Phi_0(\{T'_l\}) \rangle = \bar{E}_G. \quad (4.10)$$

Hence, we have

$$\begin{aligned} &\langle \Phi(\{T_l\}) | \mathcal{H} | \Phi(\{T_l\}) \rangle - \langle \Phi_0(\{T'_l\}) | \mathcal{H} | \Phi_0(\{T'_l\}) \rangle \\ &\geq \Delta \tilde{E}_{i,n}(\{T_l\}, \{T'_l\}) + \frac{\lambda}{2} D_{i,n}(\{T_l\}, \{T'_l\}), \end{aligned} \quad (4.11)$$

where

$$D_{i,n}(\{T_l\}, \{T'_l\}) = \sum_{l=i}^{i+n-1} (T_l + 1)T_l - \sum_{l=i+1}^{i+n-2} (T'_l + 1)T'_l, \quad (4.12)$$

$$\Delta \tilde{E}_{i,n}(\{T_l\}, \{T'_l\}) = \tilde{E}_G(\{T_l\}_{i,n}) - \tilde{E}_G(\{T'_l\}_{i+1,n-1}). \quad (4.13)$$

If rhs of (4.11) is positive, then lhs is also positive and  $|\Phi(\{T_l\})\rangle$  is not a ground state. If  $D_{i,n}(\{T_l\}, \{T'_l\}) > 0 (< 0)$ , this condition gives a lower (upper) bound of  $\lambda$  for which  $|\Phi(\{T_l\})\rangle$  is *not* a ground state.

Using the finite-size DMRG results with  $m = 240$  for  $n = 11$ , we find that the Haldane phase is not the ground state for  $\lambda \gtrsim 2.6716$  and  $\lambda \lesssim 0.86569$ , the  $F_{1/6}$  phase is not the ground state for  $\lambda \gtrsim 1.3698$  and  $\lambda \lesssim 0.47135$ , and the  $F_{1/3}$  phase is not the ground state for  $\lambda \gtrsim 1.2124$  as summarized in Fig. 4. The convergence with respect to  $m$  is confirmed.

## 5. Numerical Results for the Phase Boundary

The ground state energy per unit cell for each configuration is numerically estimated as follows:

$$\begin{aligned} \epsilon_G(\infty, \{\dot{1}\}, \lambda) &= 2\tilde{\epsilon}_G(\{\dot{1}\}) - \lambda \\ &\simeq -2.8030 - \lambda, \end{aligned} \quad (5.1)$$

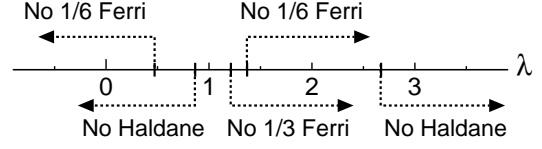


Fig. 4. Upper and lower bounds for the phase boundaries estimated from the condition that the rhs of (4.11) is positive with  $n = 11$ .

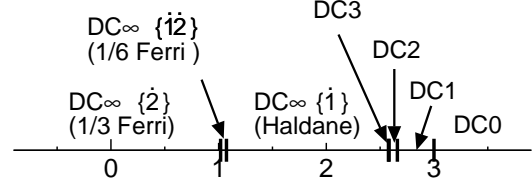


Fig. 5. Ground state phase diagram.

$$\begin{aligned} \epsilon_G(\infty, \{\dot{1}\dot{2}\}, \lambda) &= 2\tilde{\epsilon}_G(\{\dot{1}\dot{2}\}) \\ &\simeq -3.8757, \end{aligned} \quad (5.2)$$

$$\begin{aligned} \epsilon_G(\infty, \{\dot{2}\}, \lambda) &= 2\tilde{\epsilon}_G(\{\dot{2}\}) + \lambda \\ &\simeq -4.8939 + \lambda, \end{aligned} \quad (5.3)$$

where  $\tilde{\epsilon}_G(\{\dot{T}_1 \dots \dot{T}_l\})$  is the ground state energy per spin of an infinite MAFH with configuration  $\{\dot{T}_1 \dots \dot{T}_l\}$ . Among them,  $\tilde{\epsilon}_G(\{\dot{1}\})$  is the ground state energy per spin for the antiferromagnetic Heisenberg chain with spin 1.<sup>14</sup> We employ the infinite size DMRG method to evaluate  $\tilde{\epsilon}_G(\{\dot{1}\dot{2}\})$  and  $\tilde{\epsilon}_G(\{\dot{2}\})$  with  $m = 480$ . The convergence with respect to  $m$  is confirmed.

The phase boundary between the Haldane phase and the  $F_{1/6}$  phase is given by

$$\lambda_{HF_{1/6}} = 2\tilde{\epsilon}_G(\{\dot{1}\}) - 2\tilde{\epsilon}_G(\{\dot{1}\dot{2}\}) \simeq 1.0727. \quad (5.4)$$

The phase boundary between the  $F_{1/6}$  phase and the  $F_{1/3}$  phase is given by

$$\lambda_{F_{1/6}F_{1/3}} = 2\tilde{\epsilon}_G(\{\dot{1}\dot{2}\}) - 2\tilde{\epsilon}_G(\{\dot{2}\}) \simeq 1.0182. \quad (5.5)$$

The results are summarized in Fig. 5 including the results of Ref. 7. These are consistent with the upper and lower bounds reported in Sect. 4.

## 6. Summary and Discussion

The ground-state phase diagram of a spin-1 diamond chain is determined. Any eigenstate of this system can be expressed using the eigenstates of finite odd-length chains or an infinite chain with spins 1 and 2. In addition to the various paramagnetic  $DCn$  phases, the Haldane phase, and the ferrimagnetic  $DCn$  phases with 1/3 and 1/6 of the saturated magnetization are found. Among them, the ferrimagnetic phase with 1/6 magnetization is accompanied by the spontaneous translational symme-

try breakdown which was not found in previous works on diamond chains. Exact upper and lower bounds for the phase boundaries are also obtained.

In real materials, the ideal diamond chain is hardly realized. Hence, it is necessary to investigate the effect of perturbations such as lattice distortion, anisotropy, and interchain coupling. Among them, the lattice distortion is expected to transform the paramagnetic  $DCn$  phases into various types of Haldane phases and ferrimagnetic phases as discussed in the mixed diamond chain in Ref. 12. The detailed results will be reported elsewhere.

In the case of larger spin magnitude, more variety of phases are expected to appear. These are left for future studies.

**Acknowledgments** The authors are grateful to H. Kikuchi for explaining the experimental results of his group prior to publication<sup>5,6</sup> and for drawing our attention to Ref. 4. The numerical diagonalization program is based on the package TITPACK ver.2 coded by H. Nishimori. Part of the numerical computation in this work has been carried out using the facilities of the Supercomputer Center, Institute for Solid State Physics, University of Tokyo, and Yukawa Institute Computer Facility in Kyoto University. This work is supported by JSPS KAKENHI Grant Numbers JP25400389 and JP26400411.

- 1) *Introduction to Frustrated Magnetism: Materials, Experiments, Theory*, ed. C. Lacroix, P. Mendels, and F. Mila (Springer Series in Solid-State Sciences, Springer, Heidelberg, 2011).
- 2) H. Kikuchi, Y. Fujii, M. Chiba, S. Mitsudo, T. Idehara, T. Tonegawa, K. Okamoto, T. Sakai, T. Kuwai, and H. Ohta, Phys. Rev. Lett. **94**, 227201 (2005).
- 3) H. Kikuchi, Y. Fujii, M. Chiba, S. Mitsudo, T. Idehara, T. Tonegawa, K. Okamoto, T. Sakai, T. Kuwai T, K. Kindo, A. Matsuo, W. Higemoto, K. Nishiyama, M. Horović, and C. Bertheir, Prog. Theor. Phys. Suppl. 159, 1 (2005).
- 4) N. Guillou, S. Pastre, C. Livage, and G. Férey, Chem. Commun. 2002, 2358.
- 5) K. Kunieda: Master Thesis, University of Fukui (2016)[in Japanese].
- 6) H. Kikuchi: private communication.
- 7) K. Takano, K. Kubo, and H. Sakamoto: J. Phys.: Condens. Matter **8**, 6405 (1996).
- 8) K. Okamoto, T. Tonegawa, Y. Takahashi, and M. Kaburagi, J. Phys. Condens. Matter **11**, 10485 (1999).
- 9) K. Okamoto, T. Tonegawa, and M. Kaburagi, J. Phys. Condens. Matter **15**, 5979 (2003).
- 10) H. Niggemann, G. Uimin, and J. Zittartz, J. Phys. Condens. Matter **9**, 9031 (1997). , *ibid.* **10**, 5217 (1998).
- 11) K. Takano, H. Suzuki, and K. Hida, Phys. Rev. B **80**, 104410 (2009).
- 12) K. Hida, K. Takano, and H. Suzuki, J. Phys. Soc. Jpn. **78**, 084716 (2009), *ibid.* **79**, 044702 (2010), *ibid.* **79**, 114703 (2010).
- 13) K. Hida and K. Takano, J. Phys. Soc. Jpn. **80**, 104710 (2011).
- 14) S. R. White and D. A. Huse: Phys. Rev. B **48**, 3844 (1993).